Using the Generalized Inverted Pendulum to generate less energy-consuming trajectories for humanoid walking

Sahab Omran, Sophie Sakka, Yannick Aoustin

Using the Generalized Inverted Pendulum to generate less energy-consuming trajectories for humanoid walking

Sahab Omran*, Sophie Sakka#, Yannick Aoustin*,

* L'UNAM, IRCCyN, CNRS,
Ecole Centrale de Nantes, University of Nantes,
1, rue de la Noë BP 92101. 44321 Nantes, France
[sahab.omran, yannick.aoustin]@irccyn.ec-nantes.fr

IRCCyN,
University of Poitiers, France.
sophie.sakka@irccyn.ec-nantes.fr

ABSTRACT

This paper proposes an analysis of the effect of vertical position of the pivot point of the inverted pendulum during humanoid walking. We introduce a new feature of the inverted pendulum by taking a pivot point under the ground level allowing a natural trajectory for the center of pressure (CoP), like in human walking. The influence of the vertical position of the pivot point on energy consumption is analysed here. The evaluation of the energy consumption is done using a sthenic criterion in a 3D dynamics simulation of the humanoid robot ROMEO (Aldebaran Robotics) and shows a consequent reduction of the robot torque solicitation with a pivot point under the ground.

Keywords: Inverted pendulum, pivot point, walking robots, energy consumption, joint torques.

1 INTRODUCTION

The linear inverted pendulum (LIP) was proposed by Kajita *et al.* to generate humanoid walking trajectories [4, 1]. This model was widely applied to various bipedal robots like HRP-2 [8], Asimo [9], and UT-Theta [10]. The main advantage of this approach is the simplicity of the dynamics and the analytical solution. The Generalized Inverted Pendulum model (GIP) [6] is a particular case of inverted pendulum models with a pivot point under the ground level in opposition to all other inverted pendulum models (for robot control or human motion) with a pivot point at ground level. It describes human normal walking from the external forces point of view, taking into account the mechanism of foot.

This work uses the GIP model [6], initially proposed to model human walking, to generate a more human inspired walking pattern of humanoid robots. The vertical component of the pivot point has been determined in a manner to minimize the energy consumed by the system.

This paper is organised as follows: First, we show that the dynamics equations system does not change if the pivot point is located under the ground or at ground level. Then, we show the effect of the vertical position of the pivot point on the inverted pendulum energy. After, we present a simulation results on the humanoid robot Romeo using trajectories with different depth of the pivot point.

2 Dynamics equation for an inverted pendulum with a pivot point under the ground

In this section, we will study the dynamics of the inverted pendulum in the general case: The CoM is not constrained to maintain a constant height during the movement and whose pivot point is located under the ground. Fig. 1 illustrates the inverted pendulum in the sagittal plane, where the mass M moves under the force f and the gravity g. The mass is connected to the ground with a massless rod. The pivot point of the pendulum is a virtual revolt joint located under the ground, z_p is its vertical component. θ is the angle between the rod and the vertical axis. The global coordinates system is defined by the forward axis $\vec{x}$, the up-ward vertical axis $\vec{z}$ and the transversal axis $\vec{y} = \vec{z} \times \vec{x}$.
The force f and the gravity create an acceleration of the CoM $[\ddot{x}\ \ddot{y}\ \ddot{z}]^\top$. Along the vertical axis z :

$$f_z - Mg = M\ddot{z} \tag{1}$$

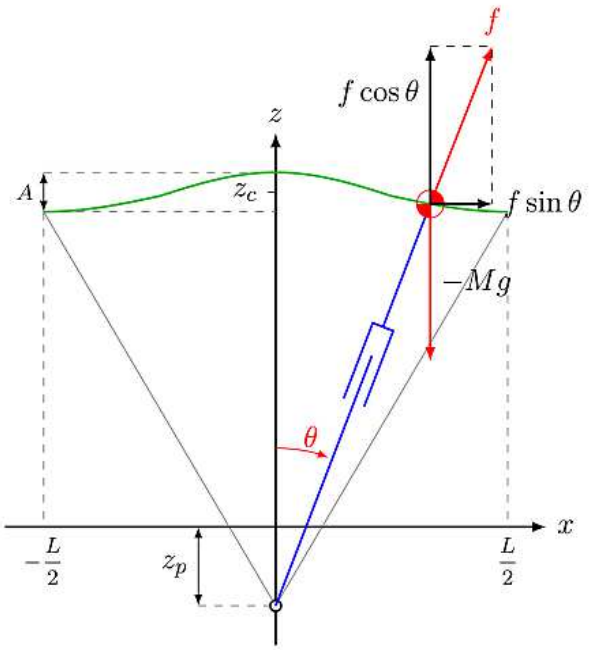

Figure 1: Generalized inverted pendulum in the sagittal plane.

$$f\cos\theta - Mg = M\ddot{z} \tag{2}$$

$$f = \frac{M(g+\ddot{z})}{\cos\theta} \tag{3}$$

Along the the forward axis x :

$$f_x = M\,\ddot{x} \tag{4}$$

$$f\,\sin\theta = M\,\ddot{x} \tag{5}$$

By substituting Eq. (3) in Eq. (5), we obtain

$$M\,(g+\ddot{z})\,\frac{\sin\theta}{\cos\theta} = M\,\ddot{x} \tag{6}$$

$$\frac{\sin\theta}{\cos\theta} = \tan\theta = \frac{x}{z-z_p} \tag{7}$$

The minus sing of z_p is justified by the fact that $z_p \leq 0$.

$$(g+\ddot{z})\frac{x}{z-z_p} = \ddot{x} \tag{8}$$

$$x = \frac{z-z_p}{g+\ddot{z}}\,\ddot{x} \tag{9}$$

In a similar manner, we obtain the motion equation in the frontal plane.

$$y = \frac{z-z_p}{g+\ddot{z}}\,\ddot{y} \tag{10}$$

The motion of the CoM is characterized by the second order differential equations (9) and (10). These equations are very similar to those in the case where the pivot point is located at ground level. The only difference is that the term z is replaced by $z-z_p$. Before the term z_p was sometimes used to express the vertical component of origin of the frame attached to the foot with respect to the global coordinate system and the pivot point was always in the foot. But now, z_p expresses the vertical distance between the pivot point and the ground. The differential equations 9 and 10 can be solved analytically when $z = const$. When $z \neq const$, these two equations are solved numerically.

3 Modeling

Let us consider a humanoid robot composed of n_{act} actuators to control its body movements in 3D. Let $\mathbf{q}$ and $\mathbf{X}$ denote the system generalized and operational coordinates vectors, respectively. We introduce the following notations:

$\mathbf{X}$	(6×1)	Absolute position and orientation of the waist ;
$\mathbf{X}_{f_i}$	(6×1)	Absolute position and orientation of foot i $(i=1,2)$;
$\mathbf{q}_{leg_i}$	$(n_{leg}\times 1)$	Actuated joints of leg$_i$ (ankle, knee and hip joints);
$\mathbf{q}$	$(n\times 1)$	Vector grouping the controlled variables $(n=n_{act}+6)$.

The vector $\mathbf{q}$ contains the joint variables and the 3D position and orientation of the frame R_0 fixed in the left foot. The reference frame is defined such that $\mathbf{x}_0$ denotes the horizontal advancement direction, $\mathbf{z}_0$ is the vertical bottom-up direction, and $\mathbf{y}_0=\mathbf{z}_0\times\mathbf{x}_0$ is the lateral direction.

3.1 Walking cycle – Assumptions

The walking cycle is defined by two successive steps (right and left legs). One step is composed of a single support phase (SS) on the stance leg, delimited by swinging foot takeoff and swinging foot strike, and a double support phase (DS) where the body weight is distributed on both legs, delimited by swinging foot strike and other foot takeoff. In what follows, the following assumptions will be considered for the complete motion:

A1 There is no rotation of the swing foot and the basin of the biped with respect to the roll, pitch, and yaw axes.

A2 The stance foot has a flat contact on the ground;

A3 Feet velocity and acceleration are equal to zero at foot strike. Thus no impact is considered.

A4 The CoM and the waist segment have the same linear velocity and acceleration profiles;

As humanoid systems are highly redundant, these assumptions allow setting the control schemes while reducing the redundancy order by setting arbitrarily several parameters. The motion of the swinging foot is defined as a polynomial function, where the polynomial coefficients were determined using initial and final positions, velocities, and accelerations.

3.2 Kinematics

For given desired Cartesian trajectories of the waist $\mathbf{X}$ and the feet $\mathbf{X}_{f_i}$ $(i=1,2)$, the inverse kinematics model leads to the values of the desired joint variables as detailed in Eq. (11).

$$\begin{bmatrix} \mathbf{V}_{f_i} \\ \omega_{f_i} \end{bmatrix} = \begin{bmatrix} \mathbf{I}_{3\times 1} & -\hat{\mathbf{L}} \\ \mathbf{0}_{3\times 1} & \mathbf{I}_{3\times 1} \end{bmatrix} \begin{bmatrix} \mathbf{V} \\ \omega \end{bmatrix} + \mathbf{J}_{leg_i}\dot{\mathbf{q}}_{leg_i} \qquad (i=1,2) \tag{11}$$

where $\dot{\mathbf{X}}_{f_i}=[\mathbf{V}_{f_i}^\top\ \omega_{f_i}^\top]^\top$, $\dot{\mathbf{X}}=[\mathbf{V}^\top\ \omega^\top]^\top$, $\mathbf{J}_{leg_i}$ $(i=1,2)$ denotes the $6\times n_{leg}$ Jacobian matrix associated to the i-th leg, $\mathbf{L}$ is the position vector between the waist and foot f_i and$\hat{}$is the skewsymetric matrix. Due to assumption **A1**, $\omega=\omega_{f_i}=0$, thus Eq. (11) becomes

$$\dot{\mathbf{q}}_{leg_i}=\mathbf{J}_{leg_i}^{-1}\begin{bmatrix}\dot{\mathbf{X}}_{f_i}-\dot{\mathbf{X}} \\ \mathbf{0}_{3\times 1}\end{bmatrix} \qquad (i=1,2) \tag{12}$$

The desired $n\times 1$ controlled velocities vector $\dot{\mathbf{q}}$ can be rebuilt as follows.

$$\dot{\mathbf{q}}=\left[\dot{\mathbf{q}}_{leg_1}\ \dot{\mathbf{q}}_{leg_2}\ \dot{\mathbf{q}}_{free}\ \dot{\mathbf{X}}\right]^\top \tag{13}$$

where $\dot{\mathbf{q}}_{free}$ denotes joint velocities of trunk and arms which can be set freely.

The rank of the Jacobian matrix of each leg was verified at each sampling period of motion to ensure that there is no singularity.

3.3 Dynamics

The dynamics of the system may be described by the three following equations.

$$\begin{cases} \mathbf{D}\ddot{\mathbf{q}} + \mathbf{C}\dot{\mathbf{q}} + \mathbf{G} = \mathbf{B}\boldsymbol{\Gamma} + \mathbf{J}_1^\top \mathbf{R}_1 & \text{if in single support, leg}_1 \\ \mathbf{D}\ddot{\mathbf{q}} + \mathbf{C}\dot{\mathbf{q}} + \mathbf{G} = \mathbf{B}\boldsymbol{\Gamma} + \mathbf{J}_2^\top \mathbf{R}_2 & \text{if in single support, leg}_2 \\ \mathbf{D}\ddot{\mathbf{q}} + \mathbf{C}\dot{\mathbf{q}} + \mathbf{G} = \mathbf{B}\boldsymbol{\Gamma} + \mathbf{J}_1^\top \mathbf{R}_1 + \mathbf{J}_2^\top \mathbf{R}_2 & \text{if in double support} \end{cases} \tag{14}$$

The matrices $\mathbf{D}(\mathbf{q})$, $\mathbf{C}(\mathbf{q},\ \dot{\mathbf{q}})$ and $\mathbf{G}(\mathbf{q})$ describe respectively the inertia, Coriolis and gravity forces acting on the system. $\boldsymbol{\Gamma}$ is the vector of the actuator torques $\boldsymbol{\Gamma}_i$, $i = 1, \cdots, nact$. The matrix $\mathbf{B}$ is the actuation matrix; it expresses the contribution of each joint torque in the virtual work δw:

$$\delta w = \boldsymbol{\Gamma}_1 \delta q_1 + \boldsymbol{\Gamma}_2 \delta q_2 + \ldots + \boldsymbol{\Gamma}_{n_{act}} \delta q_{n_{act}} = \delta \mathbf{q}^\top \mathbf{B}\boldsymbol{\Gamma}$$

where $\boldsymbol{\Gamma} = \begin{bmatrix} \boldsymbol{\Gamma}_1 \ \boldsymbol{\Gamma}_2 \ \ldots \ \boldsymbol{\Gamma}_{n_{act}} \end{bmatrix}^\top$ and $\mathbf{B} = \begin{bmatrix} \mathbf{0}_{n_{act}\times 6} \ \mathbf{I}_{n_{act}} \end{bmatrix}^\top$. The vectors $\mathbf{R}_1$ and $\mathbf{R}_2$ are the ground reaction forces exerted on foot$_1$ and foot$_2$ respectively.

$$\mathbf{R}_1 = \begin{bmatrix} R_{1x}\, R_{1y}\, R_{1z}\, M_{1x}\, M_{1y}\, M_{1z} \end{bmatrix}^\top \qquad \mathbf{R}_2 = \begin{bmatrix} R_{2x}\, R_{2y}\, R_{2z}\, M_{2x}\, M_{2y}\, M_{2z} \end{bmatrix}^\top$$

In single support, there are n unknown variables which are the components of $(\boldsymbol{\Gamma}, \mathbf{R}_1)$ or $(\boldsymbol{\Gamma}, \mathbf{R}_2)$ depending on which foot is in contact with the ground. So, the n independent equations in the two first lines of Eq. (14) are sufficient for solving. On the other hand, in double support there are $n+6$ unknown variables in $(\boldsymbol{\Gamma}, \mathbf{R}_1, \mathbf{R}_2)$ and only n equations available. In order to solve the problem in double support, six variables should be chosen and set to completely describe the system dynamics. The variables we choose are the six components of the ground reaction forces exerted on the foot that was supporting before the considered double support. Similarly to Omran *et al.* [5], these components are defined as third-order polynomial functions of time ensuring the continuity of the ground reaction forces with the two single support phases around the considered double support.

4 Energy consumption

Many criteria exist to evaluate energy consumption of a mechanical system, however to our best knowledge there is no ideal criterion [3]. In this approach, we chose the sthenic criterion which is defined by the integral of the quadratic actuators torques per unit of distance, as shown in Eq. (15). Its physical meaning is to be an image of the Joule effects if the actuators are DC motors. Furthermore, the torque amplitudes are decreased with the minimization of this criterion [2]. Then if we design an optimal walking gait with this criterion we can limit the weight of the needed motors.

$$C_\Gamma = \frac{1}{d} \int_{t_0}^{t_f} \boldsymbol{\Gamma}^\top \boldsymbol{\Gamma} \mathrm{d}t \tag{15}$$

where t_0 and t_f denote the beginning and ending instants of the total observed motion, d is the travelled distance. The sthenic criterion is a quantity proportional to the energy solicitation by actuators per unit of distance, while the quadratic torque deals with the instantaneous norm of motor torques: $E_0(t) = \boldsymbol{\Gamma}^\top \boldsymbol{\Gamma}$.

5 Simulation settings

For the validation of method, we use the model of the 33 degrees-of-freedom (dof) humanoid robot ROMEO[7]. The robot total weight is 40.53 kg and its height is 1.43 m. ROMEO dof are distributed as follows: 6 per leg, 1 for each toe, 7 per arm, 1 for the trunk, 2 for the neck and 2 for the head. As we focus on the locomotion, only the 12 dof of the legs were controlled in motion and the other dof were set to zero. The kinematic chain of the lower body of Romeo is shown in Fig. 2. To show the effect of the vertical position of pivot point, the robot performs one step

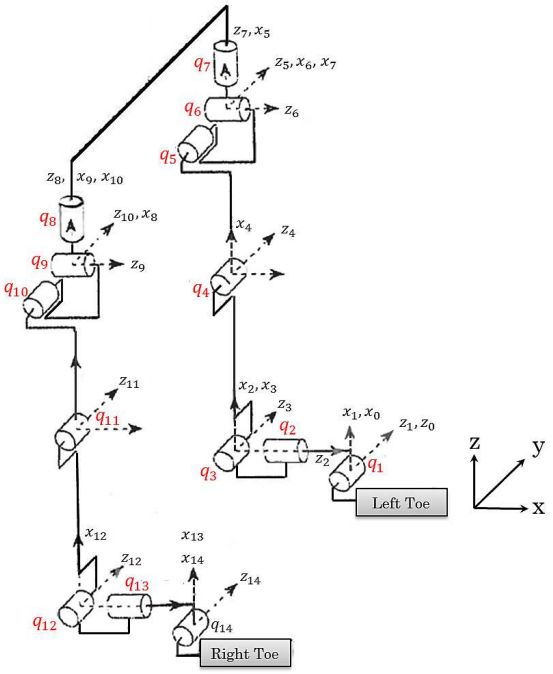

Figure 2: Lower body of humanoid robot Romeo.

forward on a flat surface. The step length is set to 0.4 m, the step width is set to 0.192 m and the step duration is 0.5 s. The height of the CoM is constant $z_c = 0.64$ m. The horizontal position of the pivot point is set in the left foot center, so the robot takes one step forward with its right foot, as shown in Fig. 3. This motion is done many times, with different depth of the pivot point

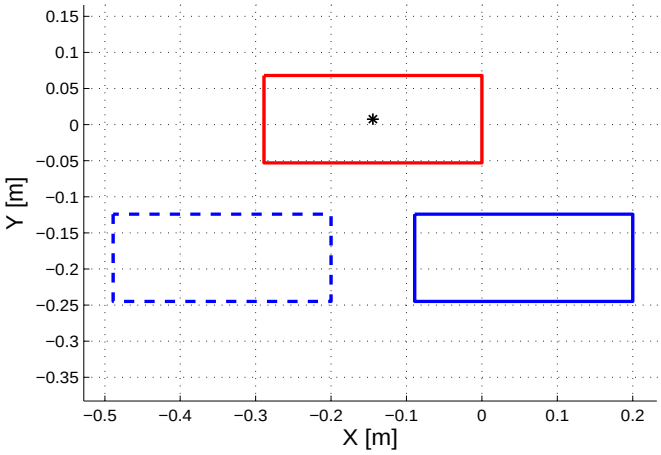

Figure 3: Feet placement for motion planing. The projection of the pivot point in the horizontal plane is represented by the black asterisk.

z_p taken in the range $[0, -1]$ m. After calculating the CoM trajectory in the horizontal plane, we obtain joint angles using the inverse kinematic model, then we calculate the joint torques using the dynamic model. In the end, we calculate the sthenic criterion for each trajectory.

6 Results

The resulting trajectories for each z_p are compared in terms of dynamic balance, joint torques and energy consumption.

6.1 Horizontal trajectory of CoM

The motion described in Sec. 5 is realized by the robot Romeo in five cases corresponding to five values of z_p: $[0, -0.25, -0.5, -0.75, -1]$ m. Fig. 4 shows the fives resulting CoM trajectories in x and y directions as a function of time. We note that the x component of the CoM comes closer to a straight line when $|z_p|$ increases. On the other hand, the oscillation amplitude of the y component decreases when the pivot point goes farther under the ground.

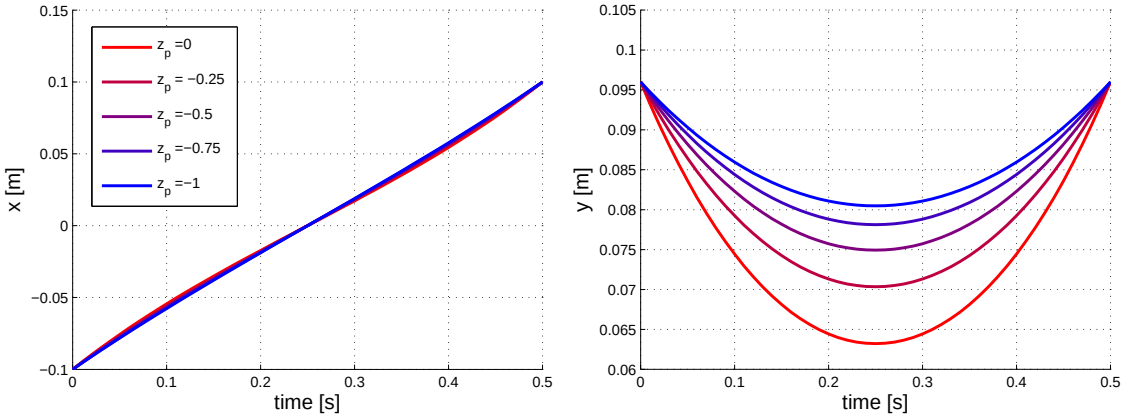

(a) Forward axis (b) Lateral axis

Figure 4: Horizontal trajectory of CoM as a function of time for five values of z_p

6.2 Trajectory of CoP

Fig. 5 represents two inverted pendulums. The first one with a pivot point at ground level ($z_p = 0$), its motion in the sagittal and frontal planes is represented in Fig. 5(a) and Fig. 5(c) respectively. The second one with a pivot point under ground level ($z_p = -1$ m), its motion in the sagittal and frontal planes is represented in Fig. 5(b) and Fig. 5(d) respectively.

In Fig. 5, the CoM is represented by circles and the CoP is represented by triangles. The ground level $(z = 0)$ is represented by a green line. We notice that the CoP coincides with the pivot point when $z_p = 0$. In this case, the CoP is a fixed point. But when the pivot point is under the ground level, the CoP moves in x and y directions as we can see in Fig. 5(b) and Fig. 5(d) respectively. For this reason, we must verify that the distances travelled by the CoP in x and y directions are smaller than the robot foot dimensions before applying the trajectory to a humanoid robot.
To describe the relation between the CoP trajectory and the depth of the pivot point, we consider three inverted pendulums having the same parameters of step length L, step width L_w, and the CoM height z_c. The pivot point depth for these pendulums are $z_{p1} = 0$, z_{p2} and z_{p3} such as $0 < |z_{p2}| < |z_{p3}|$. These three pendulums are illustrated in Fig. 6 in the sagittal and frontal planes. The foot is also represented in this figure by a bold green line.

We notice that the travelled distance by the CoP in x direction, increases when the pivot point depth increases ($L_2 < L_3$). Along the y direction, the CoP does not move when the pivot point is at ground level, but it moves in a range when the pivot point is under the ground. The range of the CoP along the y axis is increasingly far from the foot center when the $|z_p|$ increases. As we can see that l_2 is closer to the foot center than l_3.

For the bigger values of $|z_p|$, the CoP trajectory may leave the foot. For example, in Fig. 6, the CoP of the pendulum corresponding to z_{p3} leaves the contact zone between the foot and the ground. Therefore, for each foot size and step length and width, there is an upper limit of $|z_p|$ that keeps the CoP inside the foot.

For a robot with feet of length L_x and width L_y, performing a step of length L and width L_w, the

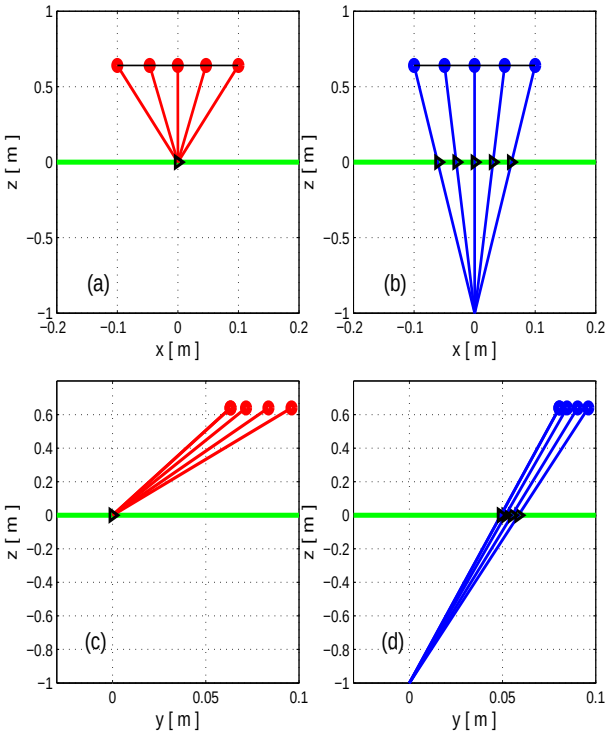

Figure 5: The inverted pendulum motion in sagittal and frontal planes in two cases: $z_p = 0$ and $z_p = -1$ m

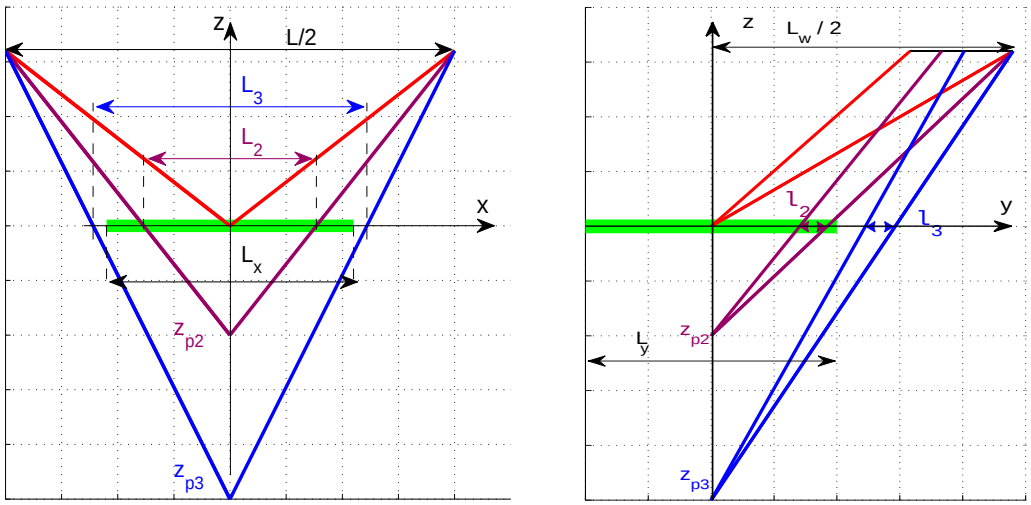

(a) Sagittal plane

(b) Frontal plane

Figure 6: The inverted pendulum during one step for three different pivot points.

upper limit of $|z_p|$ respects the following relation:

In the sagittal plane:

$$\frac{2L_x}{L} = \frac{|z_{p,max}|}{|z_{p,max}| + z_0} \qquad \text{if} \quad L > L_x \tag{16}$$

In the frontal plane:

$$\frac{L_y}{L_w} = \frac{|z_{p,max}|}{|z_{p,max}| + z_0} \qquad \text{if} \quad L_w > L_y \tag{17}$$

From these two equations, we can deduce the limit of z_p.

$$|z_{p,max,sagittal}| = \frac{2\,L_x\,z_0}{L - 2\,L_x} \qquad |z_{p,max,frontal}| = \frac{L_y\;z_0}{L_w - L_y} \tag{18}$$

The upper limit of $|z_p|$ is chosen as:

$$|z_{p,max}| = min(|z_{p,max,sagittal}|, |z_{p,max,frontal}|) \tag{19}$$

When we generate trajectories for experiments on a real robot, we should consider a security margin for CoP before calculating $|z_{\mathrm{p,max}}|$. The security margin can be defined as a percentage of foot dimensions. In simulation, the security margin may be not considered.

The humanoid robot Romeo feet are 0.289 m in length and 0.121 m in width. By applying Eq. (19), we obtain: $|z_{\mathrm{p,max}}|$ = 1.09 m. If we consider a margin of security of 50% of the foot, we obtain $|z_{\mathrm{p,max}}|$ = 0.29 m. The robot foot with the security margin is illustrated in Fig. 7.

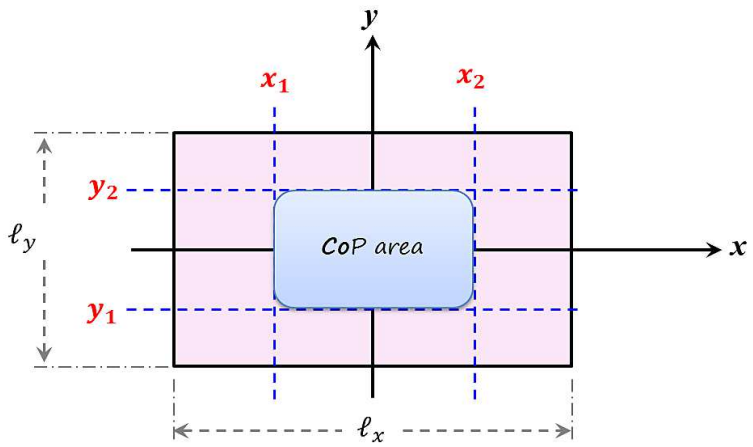

Figure 7: The foot and the CoP area.

6.3 Joint torque

In this section, we consider two trajectories for humanoid robot Romeo. The first one was calculated using an inverted pendulum with a pivot point at ground level (z_p=0) and the second one was calculated using an inverted pendulum with a pivot point under the ground ($z_p = -z_{\mathrm{p,max}}$ = -0.29 m). The two inverted pendulums have the same parameters for step length, step width, step duration and CoM height as given in Sec. 5. We compare joint torques for these two trajectories.

Fig. 8 shows the torques at the legs joints. The support leg contains six joints: ankle roll (Γ_2), ankle pitch (Γ_3), knee pitch (Γ_4), hip pitch (Γ_5), hip roll (Γ_6), and hip yaw (Γ_7). The swing leg contains six joints also: ankle roll (Γ_{13}), ankle pitch (Γ_{12}), knee pitch (Γ_{11}), hip pitch (Γ_{10}), hip roll (Γ_9), and hip yaw (Γ_8). In global, the two trajectories show similar behaviour. We can see that Γ_5, Γ_{10}, Γ_{11}, and Γ_{12} are almost the same. For these joints, the torque is a little reduced (between 1.8% and 5.2%) with a pivot point under the ground than with a pivot point at ground level.

For Γ_3, Γ_4, Γ_7, Γ_8, and Γ_9, we can observe two or three peaks for each torque. The torque amplitude peak-to-peak is reduced for $z_p = -z_{\mathrm{p,max}}$ compared to the case $z_p = 0$ by 20%, 10.8%, 1.3%, 20.2% and 26% respectively.

We can notice that main differences happen at ankle roll for the two legs Γ_2 and Γ_{13}. Γ_2 is reduced when $z_p = -0.29$ m compared to $z_p = 0$, we give the reduction rate at three moment within the

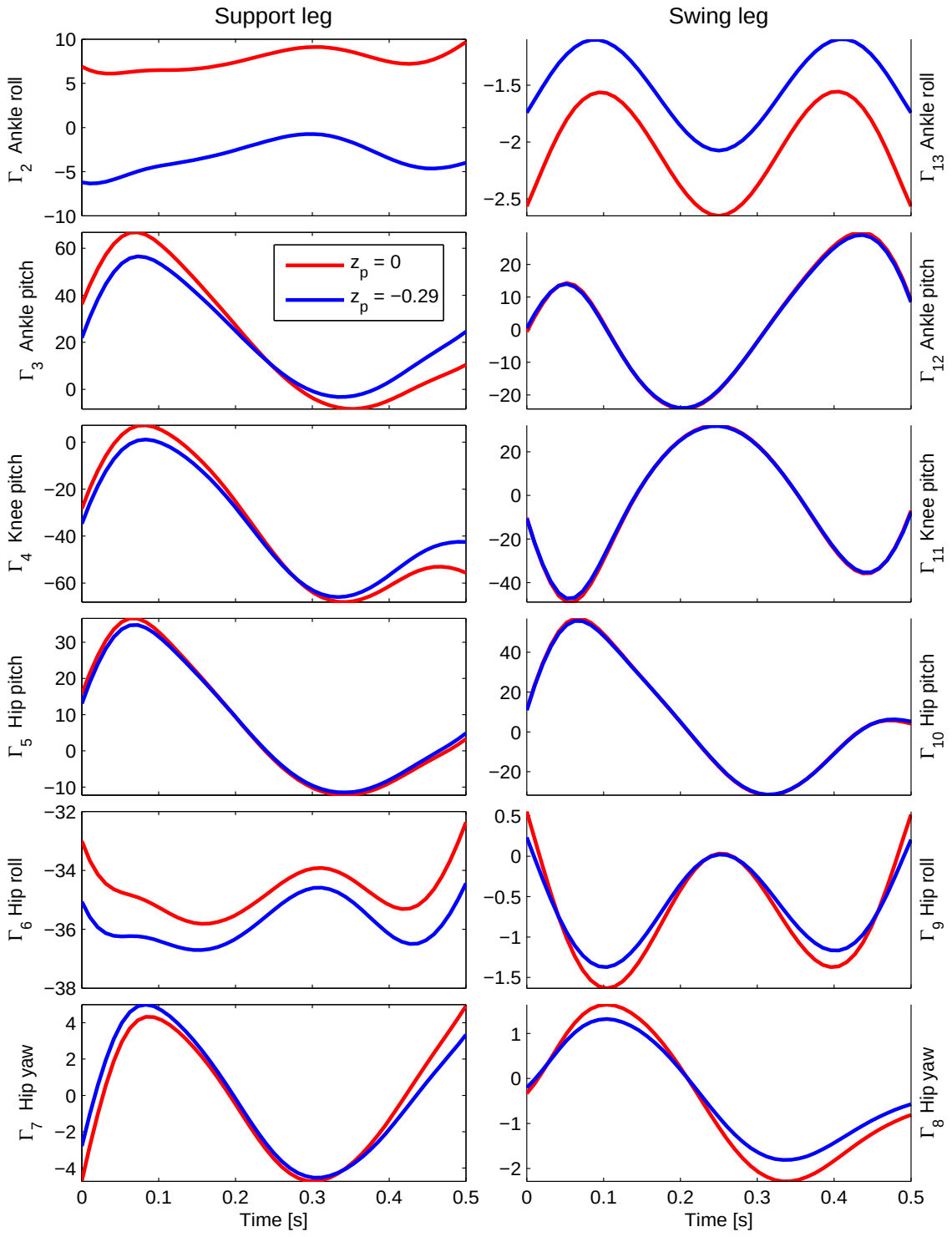

Figure 8: Joint torques for legs joints of Romeo for 2 values of the pivot point depth

motion: 9.8% at (t=0 s), 91% at the peak (t=0.31 s) and 58.8% at the end of the step (t=0.5s). In the same manner, Γ_{13} is also reduced when $z_p = -0.29$ m compared to $z_p = 0$, we give the reduction rate at the three peaks: 29.4% at (t=0.1 s), 21.6% at (t=0.25 s) and 29.5% at (t=0.4 s).

The torque at the hip roll of the support leg Γ_6 is the only one that increases when the pivot point is under the ground level. The rate of increase with respect to the case $z_p = 0$ is given at three moment within the motion: 6.22% at (t=0s), 1.97% at (t=0.31s) and 6.39% at (t=0.5s).

6.4 Energy evaluation

The profile of the quadratic torque $E_0 = \Gamma^\top \Gamma$ during one step is shown in Fig. 9. The simulations were run with two values of the pivot point depth: $z_p = 0$ and $z_p = -0.29$ m. The two graphs of

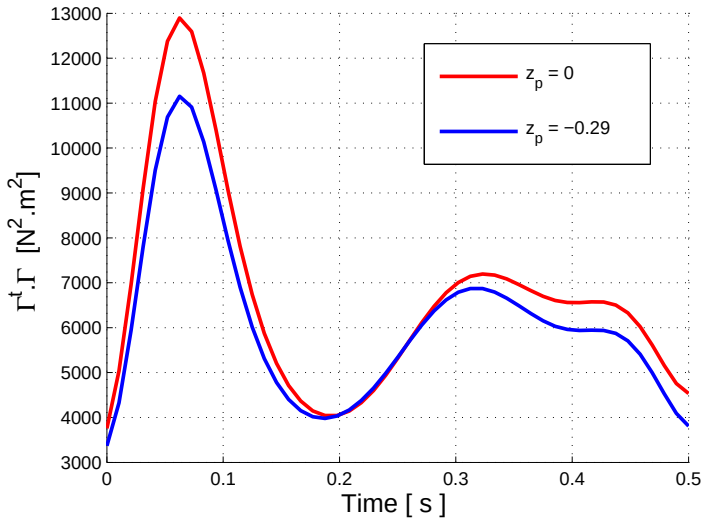

Figure 9: Quadratic torque

Fig. 9 show a peak of value at the beginning of single supports followed by a valley at midstance. Fig. 9 shows that E_0 values at the beginning and at the end of the single support are lower with a pivot point under the ground level that with a pivot point at ground level. The evolution of

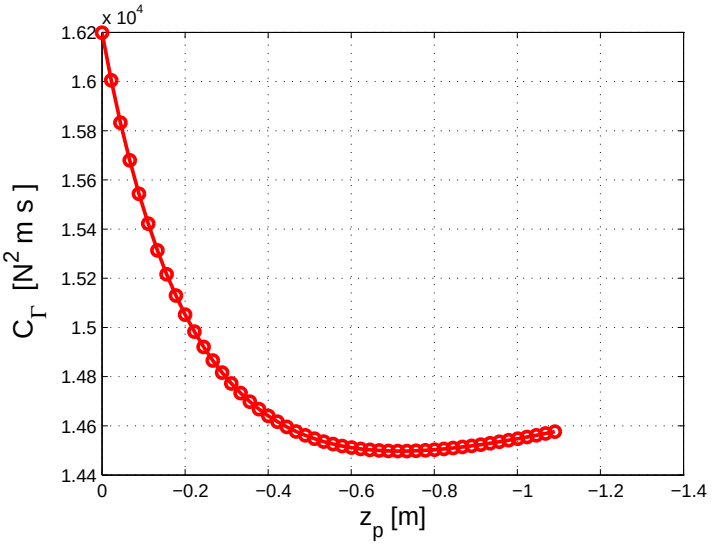

Figure 10: Sthenic criterion

the sthenic criterion as a function of the pivot point depth is shown in Fig. 10, for values of z_p between $[0 \; -1.09]$ m, which is the maximum authorized in simulation. The situation $z_p = -0.718$ m minimizes the sthenic criterion, with the criterion value being reduced by 10.5% in comparison to the case $z_p = 0$. When we consider a security margin of 50% of foot dimensions, $z_{\text{p,max}} = -0.29$ m corresponds to 9% reduction of the sthenic criterion compared to the case $z_p = 0$.

7 CONCLUSIONS

This paper proposed an analysis of the effect of the vertical position of the pivot point on the energy consumption for humanoid walking gait. A 3D simulation was proposed to compare the classical inverted pendulum with a pivot point on the ground level and an inverted pendulums with a pivot point under the ground level. The dynamics analysis showed that the use of a pivot point under the ground reduced considerably the torque solicitation especially in the beginning of the single support. Moreover,the sthenic energy can be minimized for an optimal pivot point depth.

The results can be included in walking pattern generators in order to reduce energy consumption during walking and to obtain a natural rolling of feet.

REFERENCES

[1] S. Kajita, and K. Tani, Study of dynamic walk control of a biped robot on rugged terrain - Derivation and application of the linear inverted pendulum mode. In Transactions of the Society of Instrument and Control Engineers. 27:177–184, 1991.

[2] Ch. Chevallereau and Y. Aoustin. Optimal reference trajectories for walking and running of a biped robot. Robotica, 19:557–569, 2001.

[3] Ch. Chevallereau, G. Bessonnet, G. Abba, and Y. Aoustin, Bipedal Robots. Wiley, 2008

[4] S. Kajita, F. Kanehiro, K. Kaneko, K. Yokoi, H. Hirukawa. The 3D Linear Inverted Pendulum mode: A simple modelling biped walking pattern generation. In Proceedings of the 2001 IEEE/RSJ International Conference on Intelligent Robots and Systems, Maui, Hawaii, USA 2001.

[5] S. Omran, S. Sakka, Y. Aoustin. Effects of the vertical CoM motion on energy consumption for walking humanoids. In Proceedings of the 17th International Conference on Climbing and Walking Robots and the Support Technologies for Mobile Machines, 2014.

[6] S. Sakka, Ch. Hayot, P. Lacouture. A generalized 3D inverted pendulum model to represent human normal walking. In IEEE-RAS International Conference on Humanoid Robots, 2010.

[7] Aldebaran Robotics. Romeo humanoid robot documentation, 2012.

[8] AIST. HRP-2. http://global.kawada.jp/mechatronics/hrp2.html, since 1998.

[9] Honda Motor Co. ASIMO. http://world.honda.com/ASIMO/, since 1996.

[10] The University of Tokyo. UT-Theta. http://www.ynl.t.u-tokyo.ac.jp/research/ut_theta/, since 2001.